ORIGINAL ARTICLE

Bardoxolone Methyl Ameliorates Hyperglycemia Induced Mitochondrial Dysfunction by Activating the keap1-Nrf2-ARE Pathway in Experimental Diabetic Neuropathy

Anil Kumar Kalvala[1] · Rahul Kumar[1] · Bhoomika Sherkhane[1] · Chayanika Gundu[1] · Vijay Kumar Arruri[1] ·
Ashutosh Kumar[1] (ORCID)

Abstract

Bardoxolone methyl (Bard), a nuclear factor erythroid 2-related factor 2 (Nrf2) activator regulates multiple oxidative and inflammatory diseases. However, the role of Bard in painful diabetic neuropathy (DN) remains unknown. Bard administration at two dose levels (15 & 30 mg/kg/day) to STZ (55 mg/kg, i.p) induced diabetic rats for last two weeks of eight week study significantly improved motor nerve conduction velocity (61.84 ± 1.9 vs. 38.57 ± 1.08 m/s), sensory nerve conduction velocity (66.86 ± 5.1 vs. 39.43 ± 3.3 m/s), nerve blood flow (86.28 ± 6.4 vs. 56.56 ± 1.62 PU), and intraepidermal nerve fiber density. Additionally, Bard treatment attenuated thermal and mechanical hyperalgesia in diabetic rats. Further molecular investigation on dorsal root ganglions (DRG) tissue isolated from L4-L6 regions of diabetic rats and High glucose (HG) exposed PC12 cells displayed decreased expression and transcriptional activity of Nrf2 which might have resulted in depleted antioxidant enzymes and mitochondrial chaperones. Bard treatment significantly reversed these effects in diabetic rats and also in HG exposed PC12 cells. Moreover, mitochondrial complex activities were diminished in DRG mitochondrial fractions of diabetic rats and mitochondrial isolates of HG exposed PC12 cells and Bard treatment significantly reversed these effects. Furthermore, Bard treatment significantly impeded the impact of hyperglycemic insults on mitochondrial membrane potential, ROS production and mitochondrial oxygen consumption rate (OCR) (Basal respiration, Maximal respiration, ATP production and spare respiratory capacity) in PC12 cells. Collectively our data suggests that Bard treatment to STZ induced diabetic rats robustly reduces DN which may be due to its effect on Keap1-Nrf2-ARE pathway and have contributed to improvement in mitochondrial function.

Keywords Bardoxolone methyl · Diabetic neuropathy · Nrf2 · Mitochondrial function

Introduction

Diabetes has reached pandemic proportions worldwide, with IDF estimates demonstrating that 425 million adults were living with diabetes currently and about 352 million people are at risk of developing diabetes. It is also projected that 625 million people will suffer from diabetes by the year 2045 [1]. Infact, the considerable morbidity, poor quality of life and mortality with diabetes is associated with diabetic complications. Diabetic Neuropathy (DN) is one of the major clinical manifestations of diabetes that affects 50–70% of the diabetic population [2]. This causes the alterations in autonomic, sensory and motor neuronal transmission. Sensory defects include numbness, paraesthesia, dysaesthesia and limb amputations which add misery to life of person suffering from long withstanding diabetes. IDF noticed that for every 30 s, loss of lower limb or a part of lower limb occurs somewhere in the world in diabetic patients [3]. Duloxetine and pregabalin are main stay therapy for the symptomatic relief of DN [4]. Non availability of drugs for treating complications like neuropathy and neuropathic pain as well as poor understanding of pathobiology of the DN necessitates the quest to research for finding newer targets/therapies to meet this unmet clinical need.

Advanced research articulates disturbances created in the normal mitochondrial maintenance by the metabolic excess during hyperglycemia induced distress in the peripheral neurons [5].

✉ Ashutosh Kumar
  ashutoshniper@gmail.com; drashutoshniper@gmail.com

1 Department of Pharmacology and Toxicology, National Institute of Pharmaceutical Education and Research (NIPER)-Hyderabad, Bala Nagar, Hyderabad TG-500037, India

Recent reports clearly evidenced the loss of mitochondrial function and impaired mitochondrial biogenesis as major culprits for DN progression [6, 7]. Accumulating literature suggests that nuclear factor erythroid 2-related factor 2 (Nrf2) play a pivotal role in regulation of mitochondrial homeostasis [8]. Nrf2 null mice showed severe mitochondrial dysfunction and perturbed mitochondrial biogenesis which was evident by compromised mitochondrial complex activities and reduced expressions of PGC-1α and mitochondrial transcription factor A (TFAM) [9, 10]. Several preclinical and clinical studies reported significant improvement in mitochondrial function by administration of Nrf2 activators [11, 12]. Further, experimental studies also revealed that Nrf2 activation curbed mitochondrial proteotoxicity by enhancing chaperones expression [13]. Recently, Nrf2-ARE elements have been reported to bind at heat shock factor 1 (HSF-1) gene and promote the expression of HSF-1 protein [14]. Sirtuin 3 (SirT3) is an NAD+ dependent deacetylase which primarily resides in mitochondria and functions to maintain mitochondrial homeostasis under stress [15]. However, Nrf2-ARE binds on promoter regions of SirT3 and regulates its transcriptional expression [16]. Mitochondrial lon protease (LONP1) plays a pivotal role in mitochondrial quality control and cellular homeostasis by eliminating abnormal proteins and concurs in rapid turnover of regulatory proteins [17]. SirT3 deacetylates LONP1 and thereby mediates its mitochondrial protective effects [18]. Decades of research in diabetes articulated that oxidative stress, inflammation, apoptosis, mitochondrial dysfunction, perturbed mitochondrial biogenesis and autophagic defects were the major culprits for the progression of DN [19].

Bardoxolone methyl (Bard) is a semi synthetic oleanane triterpenoid derivative which has been studied in clinical trials against diabetic nephropathy owing to its potential antioxidant and anti-inflammatory properties [20]. This drug effects were investigated in the patients suffering from diabetic nephropathy (BEAM TRIAL) and it was observed to ameliorate renal function [21]. Later, BEACON (Phase 3 trial) observed similar renoprotective actions, but it was terminated for adverse events precipitated to cardiac failure [22]. However, a new study reported Bard might be safe with patients without cardiovascular risk [23]. Bard conjugates with cysteine residues available on kelch-like ECH-associated protein 1 (Keap1) and allows Nrf2 translocation into the nucleus and thereby regulates Nrf2 transcriptional activities in controlling cellular homeostasis [24]. Several preclinical studies also reported the protective effects of Bard against multiple diseases by targeting Nrf2 activation in controlling oxidative stress and inflammation [25].

In the present study we evaluated the neuroprotective potential of Bard by targeting Keap1-Nrf2-ARE pathway, in regulation of mitochondrial function, mitochondrial biogenesis and proteotoxicity under diabetic condition using in vivo and in vitro systems.

Materials and Methods

Chemicals and Kits

Unless specified all the chemicals were of reagent grade and obtained from Sigma Aldrich, USA. Bard is obtained from MedChem Express, USA. Complex I (ab109721), IV (ab109911) and V (ab109714) activity assay kits were purchased from Abcam, UK. RPMI 1640 media is purchased from Invitrogen.

Animals

Three months old (250–270 g) Healthy Male Sprague Dawley (SD) rats were fed on standard diet and water ad libitum and housed in plastic cages (temperature $24 \pm 1°c$, humidity $55 \pm 5\%$) with 12 h light-dark cycle. All the experiments were conducted as per guidelines laid by Committee for the Purpose of Control and Supervision of Experiments on Animals (CPCSEA) guidelines and Institutional Animal Ethics Committee (IAEC)-NIPER Hyderabad.

Diabetes Induction and Experimental Design

After 2 h fasting, diabetes was induced by single dose of STZ (55 mg/kg, i.p.) in a citrate buffer (pH 4.5). Blood samples were collected from tail vein 48 h after STZ administration. Rats with plasma glucose levels more than 250 mg/dl were considered as diabetics and considered further for study. Diabetic animals were randomized into three groups comprising of diabetic control group (STZ-D), diabetic rats treated with 15 mg/kg Bard (STZ-D + Bard15) and 30 mg/kg Bard (STZ-D + Bard30). Age matched control rats were randomized into two groups namely non diabetic animals (ND), treatment control (Bard30) receiving 30 mg/kg Bard. The treatment was started 6 wk. after diabetes induction and was continued for 2 wk. as shown in Fig. 1. Bard was dissolved in sterile saline and 1% tween 80 as a vehicle [26]. The functional and biochemical parameters were performed 24 h after administration of last dose. Biochemical and molecular studies were performed on isolated dorsal root ganglions (DRG) from L4-L6 origin.

PC12 Cell Culture

Rat pheochromocytoma (PC12) cell line was purchased from NCCS, Pune, India and were cultured in RPMI 1640 media supplemented with 10% FBS, glutamine (2 mM), streptomycin/ penicillin (1%), glucose (5.5 mM) and grown at 37 °C, in a humidified atmosphere of 95% air and 5% CO2. Prior to the experiment, cells were differentiated with 50 ng/ml of nerve growth factor (NGF) in serum free media for 24 h (18). High glucose (HG) condition was simulated by
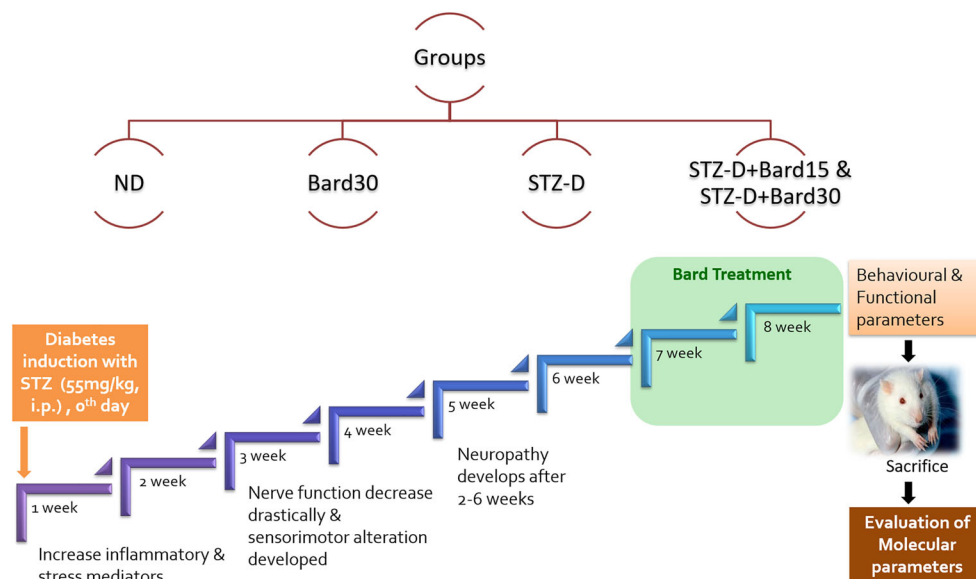
Fig. 1 Flow chart representing the experimental design. Single dose of STZ administration (55 mg/kg, i.p) to SD rats induced diabetes. Diabetic neuropathy was conformed in 6 wk. after Diabetes induction. Bard at the dose 15 and 30 mg/kg of body weights of rats were administered to animals for 2 wk. after conforming diabetic neuropathy. Last dose after 24 h, animals are subjected to behavioral, functional and biochemical assessment. ND: Non diabetic, Bard30: Non diabetic rats treated with Bardoxolone methyl at 30 mg/kg, STZ-D: Diabetic, STZ-D + Bard15 & STZ-D + Bard30 are Diabetic rats treated with Bardoxolone methyl at 15 and 30 mg/kg respectively

exposing PC12 cells to 30 mM β-D glucose. This glucotoxic concentration (30 mM) was previously standardized to simulate in vivo diabetic condition in many in vitro models of diabetic complications [5]. Based on MTT results obtained, we have chosen 0.25 and 0.5 μM of Bard (IC50: 1.67 μM) as a sub maximal doses to assess its neuroprotective potential in HG exposed PC12 cells. We had considered 6 h time point to study the effects of Bard on ROS or mitochondrial superoxide production and 24 h time point to study the molecular parameters [5].

Nerve Functional Studies

Nerve Conduction Velocity (NCV)

MNCV and SNCV were assessed in the sciatic-posterior tibial conducting system using the Power Lab 4sp system (AD Instruments, Australia) as described previously. Briefly, the sciatic nerve was stimulated proximally at the level of sciatic notch and the time taken to receive the electrical impulse distally at the level of ankle of the rats was measured as NCV. The time for first deflection and second deflection in the lab chart software was considered as respective time latencies to determine the MNCV and SNCV in m/s units [27].

Nerve Blood Flow (NBF)

Sciatic NBF was determined by Laser Doppler Oxymeter (Moor Instruments, UK) as described in our previous reports. Briefly, a laser probe was placed over the left flank of cut

opened sciatic nerve of anesthetized animals and flux was measured for 10 min using moor instrument software. Average arbitrary perfusion units were recorded among the different group of animals [28].

Behavioral Parameters

Thermal and Mechanical Hyperalgesia

Thermal hyperalgesia was determined by using Hargreaves plantar apparatus. Time taken for a rat to lift the paw during infrared irradiation (40%) was recorded in the system connected software with a cut off time of 20s and five consecutive readings were taken and each reading reported as paw withdrawal latency in seconds [29]. Thermal sensitivity of the rat was also measured using hot (45 °C) and cold water tail immersion (10 °C) tests in which the time latency for the animal to flick its tail was measured with cut off time 15 s and three consecutive readings were taken with an interval of 30s among each reading reported as paw withdrawal latency in seconds [30].

Mechanical hyperalgesia was measured using Vonfrey Aesthesiometer and Randall Sellito Calipers (IITC life sciences, USA). The force at which paw withdrawal of the animal was observed indicates paw withdrawal threshold in grams. Five consecutive readings were taken with at least 5 min interval among each read point. The average of the paw withdrawal threshold was calculated from the observations [31].

Biochemical Parameters

Measurement of Plasma Glucose Levels

Tail blood vein of rats was centrifuged at 5000 RPM for 5 min to separate plasma in a 1 ml heparinized centrifuge tubes and GOD-POD kit (Accurex, India) was used to estimate plasma glucose in mg/dl as per the manufacturer protocol [19].

Isolation of Mitochondria

Mitochondria from DRG tissue (MITOISO1, Sigma) and PC12 cells (MITOISO2, Sigma) were isolated using the kits according to the manufacturer protocol.

Enzymatic Activity

Enzymatic activities of mitochondrial complex I (ab109721, Abcam), IV (ab109911, Abcam) and V (ab109714, Abcam) were measured in the freshly prepared mitochondrial samples of DRG and PC12 cells using the kits according to the manufacturer protocol. Briefly, DRG and PC12 cells were minced in ice cold conditions using the mitochondrial isolation buffers provided in kit containing protease and phosphatase inhibitor cocktail (1:100). 40 µg of protein sample was used to perform this assay. Absorbance was recorded using spectrophotometer (Molecular Devices, CA, USA) at specified wavelengths as indicated in manufactures protocol [32].

GSH Activity Assay

Reduced GSH was measured by Ellman's method in DRG homogenates of diabetic rats with slight modifications. Briefly, 5% Trichloroacetic acid was used to precipitate out the proteins. To the supernatant, 100 µl of Ellman's reagent (dithiobis 2- nitro benzoic acid (DTNB)) in potassium dihydrogen phosphate buffer (pH: 8) was added. The resulting mixture was then incubated for 10 min at 37°c and the absorbance was measured at 412 nm [33].

Estimation of ATP Levels

ATP levels in DRG tissue was estimated according to the kit protocol (calorimetric assay, MAK190). The concentration of ATP was expressed in nmol/mg protein as reported elsewhere [19].

Protein Expression Studies

Immunohistochemistry (IHC)

Briefly, deparaffinized rehydrated micro sections (5 µm) of DRG were heated in citrate buffer (pH: 6.0) for antigen retrieval. Endogenous peroxidase activity was inhibited by incubating the sections with 3% H_2O_2 solution, then blocked with 3% BSA in PBS for 60 min followed by Nrf2 antibody incubation at a dilution of 1:200, (Santacruz biotechnologies, USA) at room temperature for 2 h. The sections were washed with tris buffered saline (pH: 7.4) followed by 30 min incubation with anti rabbit secondary antibody (1:100), at room temperature. Chromogenic staining was carried out with VECTASTAIN® Elite ABC Reagent kit (Vector Labs, CA, USA) according to the instructions provided in the kit until the development of desired brown intensity. Sections were counterstained with hematoxylin followed by dehydration and then mounted with DPX. At least 5 different microscopic fields in each section were observed under light microscope (Olympus corporation, Japan) to ascertain the immunopositivity [34].

Immunofluorescence

Deparaffinized, rehydrated DRG micro sections were heated in citrate buffer (pH: 6.0) for antigen retrieval followed by blocking with 3% BSA, the cells were then incubated with rabbit SOD2 Ab (1:200 dilution), rabbit SirT3 (1:50) and with rabbit LONP1 Ab (1: 50 dilution) at 4 °C for overnight. After PBS washing they were incubated for 2 h with anti rabbit rhodamine (1:100) or anti rabbit FITC (1:100) conjugated secondary antibodies at room temperature. Sections were then mounted with DAPI containing mounting medium (sigma) and observed under confocal microscope (Leica TCS SP8 Laser Scanning Spectral Confocal, Germany) [35].

Immunocytochemistry

For detailed procedure, please refer to the protocol mentioned elsewhere (24). Briefly, cells were plated at an appropriate cell density on glass cover slips placed in 6-well plates and subjected to different treatment conditions. Following 24 h after treatment, media from the wells was removed and cells were fixed in 4% paraformaldehyde for 5 min. Cells were then permeabilized with 0.5% Triton-X 100 for 10 min at room temperature and then subjected to blocking with 3% BSA for 2 h. Later, cells were incubated with primary antibodies; Nrf2 (1:200) in 3% BSA at 4 °C for overnight followed by incubation with secondary anti rabbit antibody conjugated with FITC (Sigma) for 2 h at room temperature. Finally the coverslips were mounted on a glass slide with a DAPI mounting medium (Fluoroshield™) (Sigma). Images were obtained using a confocal microscope (Leica TCS SP8 Laser Scanning Spectral Confocal) [5].

Western Blotting

DRG protein lysates prepared in tissue protein extraction reagent (TPER, Sigma) and protein lysates from PC12 cells were prepared in radioimmunoassay buffer [36]. The homogenate was centrifuged at 12000 g for 20 min at 4 °C and the clear supernatant was isolated and determined for protein content by Bradford assay. Equal quantity of protein samples was resolved using SDS-PAGE gel electrophoresis and transferred on to the PVDF / nitrocellulose membrane followed by blocking with 5% non fatty dried milk powder / 3% BSA solution in TBST. The membranes were incubated with primary antibodies at 4 °C overnight; Keap-1, SOD2, HSF1, HSP27, HSP90, HSP60, HSP27, SirT3 and LONP1 obtained from cell signaling technology (CST), USA, Nrf2, HO-1 and NQO1 procured from Santacruz biotechnologies, USA, ATP synthase c and Complex 1 purchased from Abcam, USA, were prepared at 1:1000 dilution in TBST. The membranes were incubated with HRP tagged secondary anti-rabbit and anti-mouse antibody for 2 h at room temperature. Luminescence signal was captured using a Fusion-FX imager (Vilber Lourmat, Germany) and relative band intensities were quantified by densitometry using image J software (version 1.48, NIH, USA) [37].

Co-Immunoprecipitation

PC12 cell lysates were prepared with Radioimmunoprecipitation buffer [36] and the primary antibody SirT3 or control rabbit 2° antibody (IgG) were coupled with Dynabeads/Protein G beads (Invitrogen, CA) and incubated 12 h at 4 °C. The Ab–Ag immunocomplex was collected after magnetic separation and three times washed with PBS. Immunocomplexes were released into 2× SDS sample buffer by boiling at 95 °C for 10 mins. Proteins were resolved on 10% SDS-PAGE gel and blocked with 3% BSA and the membrane was incubated with the primary antibodies SirT3 and LONP1 for 12 h at 4 °C, followed by incubation with an HRP-conjugated secondary antibody for 2 h. Luminescence signal was captured using a Fusion-FX imager (Vilber Lourmat, Germany) and relative band intensities were quantified by densitometry using image J software (version 1.48, NIH, USA) [38]. Co-immunoprecipitation of LONP1 and SirT3 experiment may evidence the expression and association among these proteins in various groups which have an immense role in the regulation of mitochondrial function.

Intra Epidermal Nerve Fiber Density (IENF) in Hind Paw

Foot pad micro sections (8 μM) were processed as described in Immunofluorescence protocol. PGP 9.5 antibody (1:200 dilution, Abcam, UK) was used to label the nerve fibers.

Confocal microscopic images were captured at 6300X using oil immersion on the slide [32].

Analysis of Mitochondrial Potential (Δψm) by JC-1 Staining

JC-1 Staining was performed on PC-12 cells as described earlier [36]. Cells were given group wise treatment and after 6 h followed by incubation for 15 min with 5 μM of JC-1. After trypsinization and centrifugation, the pellets were resuspended in PBS containing 5% FBS and subjected to fluorescence analysis using BD FACSVerse (BD Biosciences, CA, USA).

Evaluation of Total ROS and Mitochondrial Superoxide Anion (O$^-$2) by Mitosox Staining

It was performed on neuronal PC-12 cells as per the previously mentioned protocol with slight modifications. After 6 h of treatment, Cells were incubated with 10 μM of DCFDA for measuring total ROS and 5 μM of Mitosox red for measuring mitochondrial superoxides for 10 mins at 37 °C in CO_2 incubator followed by PBS washing. After trypsinization and centrifugation, the pellets were resuspended in FBS containing PBS and subjected to fluorescence analysis using BD FACSVerse (BD Biosciences, CA, USA) [5].

Extracellular Flux Analysis to Measure Mitochondrial Respiration

Mitochondrial respiration was measured by using Seahorse XFp analyzer (Agilent technologies, USA). XFp analyzer designed with a transient 7 μl chamber in a specialized 8 well microplates allows measuring oxygen consumption rate (OCR) in real time. Briefly, neuronal cell density was maintained between 4000 and 5000 cells per well leaving A and H control wells. The cells were differentiated, transfected and treated according to the experimental design. One hour before measurement of OCR, RPMI 1640 media was changed with Dulbecco's modified eagle medium with 1 mM pyruvate and 2 mM glutamate. Oligomycin (1 μM); FCCP (Carbonyl cyanide-p-trifluoromethoxyphenylhydrazone) (2 μM); and rotenone + antimycin A (1 μM each) were injected sequentially through ports in the Sea- horse flux pak cartridges. Each loop was started with mixing for 3 mins, delayed for 2 mins and followed measuring OCR for 3 mins. This experiment allows to measure the amount of oxygen consumption linked to ATP production, spare respiratory capacity, basal respiration and maximal respiration in respective wells. The data was imported into wave software and it allowed us to measure all aforementioned parameters after normalizing with the protein concentration of respective wells. The data was represented as OCR picomoles/min/mg/ml protein [5].

Statistical Significance

The values are represented as mean ± SEM. The inter-group variation was measured by one way ANOVA followed by "Bonferroni's Multiple Comparison Test" using the Graph Pad Prism, version 5.0. Results with p values <0.05 were considered to be statistically significant.

Results

Bard treatment for two weeks at dose levels of 15 and 30 mg/kg has insignificant effect on blood glucose levels and body weights of STZ induced diabetic rats. Body weights and blood glucose levels of diabetic rats were significantly ($p < 0.001$) altered when compared to age matched normal control rats (Table 1).

Effect of Bard Treatment on Nerve Function and Neurobehavior of Diabetic Rats

Eight weeks after, STZ induced type 1 diabetic rats have shown significantly ($p < 0.001$) reduced MNCV, SNCV and NBF when compared to age matched normal control rats (Fig. 2). Last two weeks of Bard treatment (15 & 30 mg/kg) to eight weeks diabetic rats significantly increased MNCV (p < 0.001), SNCV (p < 0.001) and NBF (p < 0.001) in a dose dependent manner when compared to diabetic rats (Fig. 2). Eight weeks old diabetic rats significantly displayed reduced thermal and mechanical insensitivity when compared to normal control rats (Table 1). Bard treatment at two dose levels significantly improved thermal and mechanical insensitivity of diabetic rats in a dose dependent pattern (Table 1). Intra epidermal nerve fiber density (IENFD) is considered as surrogate marker for identifying peripheral neuropathy. IENFD significantly decreased in the epidermis of hind paw microsections of diabetic rats when compared to normal control rats. Bard treatment (30 mg/kg) for two weeks to diabetic rats significantly improved IENFD in hind paws as shown in the Fig. 2.

Effect of Bard Treatment on Oxidative Stress and Heat Shock Response

IHC analysis of Nrf2 expression in DRG micro sections revealed reduced expression of Nrf2 in diabetic rats when compared to normal control rats (Fig. 3A). Nrf2 expression was significantly increased in DRG micro sections of Bard (30 mg/kg) treated diabetic rats (Fig. 3A). Further, immuno-colocalization study of Nrf2 revealed that the expression and colocalization of Nrf2 into the nucleus was decreased (Fig. 6A) in high glucose (HG) exposed PC12 cells after 24 h. When HG exposed PC12 cells were treated with 0.5 μM Bard, Nrf2 expression and colocalization into the nucleus was enhanced when compared to hyperglycemic PC12 cells (Fig. 6A). Further western blotting analysis revealed that protein expressions of Nrf2, SOD2, NQO1, HO-1, HSF-1, HSP27, HSP60, HSP90 and HSP70 significantly decreased in DRG homogenates of diabetic rats (Fig. 3B & C) and High glucose exposed PC12 cell lysates (Fig. 6B & C). These protein expressions significantly increased in DRG homogenates of diabetic rats after treatment with Bard at two dose levels (15 & 30 mg/kg) (Fig. 3B & C) and in Bard treated (0.25 and 0.5 μM) hyperglycemic PC12 cells (Fig. 6B & C) in a dose dependent manner. To confirm further, we performed IF assay for SOD2 expression in DRG microsections of diabetic rats. SOD2 expression are enhanced in DRG microsections of Bard treated diabetic rats (Fig. 3A) and which was under expressed in DRG microsections of diabetic rats when compared to control rats (Fig. 3A).

Table 1 Table 1. **Effect of two oral administration of Bard (15 & 30 mg/kg) on various behavioral and biochemical deficits of STZ induced DN:** Values are expressed as mean ± SEM ($n = 3$–6). ND: Non diabetic, Bard30: Non diabetic rats treated with Bardoxolone methyl at 30 mg/kg, STZ-D: Diabetic, STZ-D + Bard15 & STZ-D + Bard30 are Diabetic rats treated with Bardoxolone methyl at 15 and 30 mg/kg respectively. *$p < 0.05$, **$p < 0.01$, ***$P < 0.001$ Vs STZ-D & ^^$p < 0.01$ and ^^^$p < 0.001$ Vs ND

| Parameter	ND	Bard30	STZ-D	STZ-D + Bard15	STZ-D + Bard30
Tail withdrawal latency to hot stimuli (s)	11.69 ± 0.32	11.32 ± 0.60	5.41 ± 0.34^^^	6.91 ± 0.61	10.08 ± 0.40***
Tail withdrawal latency to cold stimuli (s)	14.08 ± 0.46	12.82 ± 0.67	6.95 ± 0.37^^^	8.81 ± 0.32	11.52 ± 0.38***
Paw withdrawal latency (s)	12.23 ± 0.60	11.86 ± 0.62	6.29 ± 0.74^^^	9.40 ± 0.60*	11.28 ± 0.51***
50% Paw withdrawal threshold (g)	12.5 ± 1.11	11.66 ± 1.0	6.66 ± 0.84^^	8.83 ± 1.37	11.2 ± 1.45*
Paw withdrawal pressure (g)	192.11 ± 2.52	187.72 ± 2.91	92.88 ± 2.59^^^	138.77 ± 3.95	163.16 ± 4.07**
Plasma glucose (mg/dl)	95.01 ± 3.12	97.13 ± 3.91	398.19 ± 6.31^^^	365.84 ± 5.11	329.43 ± 9.43
Average Body weight (g)	389.21 ± 9.66	384 ± 4.37	215.98 ± 4.87^^^	226.95 ± 5.19	253.81 ± 6.18
GSH (μM/mg)	24.66 ± 1.83	28.98 ± 0.96	14.73 ± 1.24^^	23.89 ± 1.39*	28.22 ± 2.0***
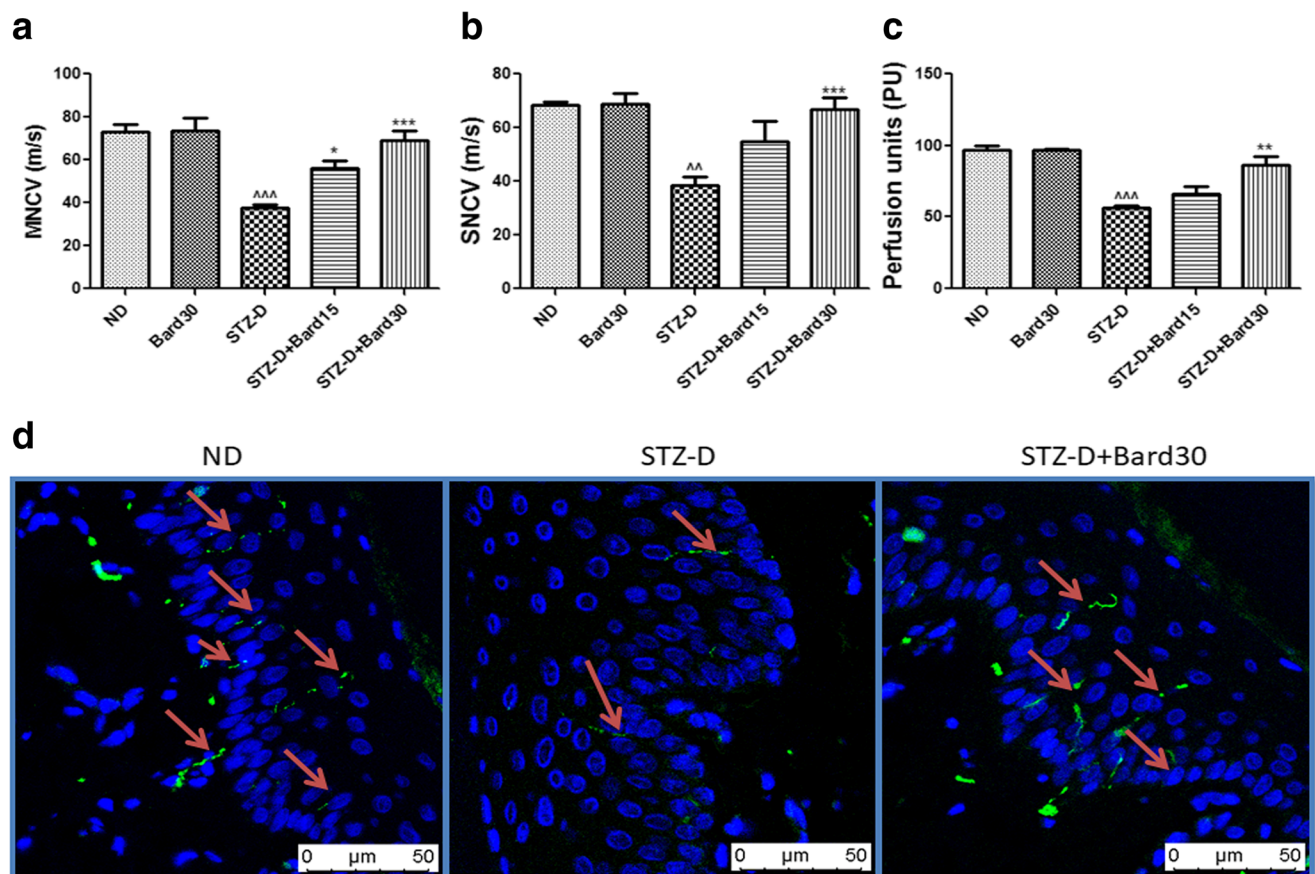
Fig. 2 Effect of Bard administration on nerve functional characteristics and intra epidermal nerve fiber density in diabetic rats. Graphical representations showing (A) motor and (B) sensory nerve conduction velocities (MNCV & SNCV), (C) nerve blood flow (NBF) in normal, diabetic and Bard treated rats. Values are expressed as mean ± SEM ($n = 6$) (D) Fluorescent images showing the expression of PGP9.5 staining in plantar skin tissue sections of normal and diabetic rats. Values are expressed as mean ± SEM ($n = 3$). ND: Non diabetic, Bard30: Non diabetic rats treated with Bardoxolone methyl at 30 mg/kg, STZ-D: Diabetic, STZ-D + Bard15 & STZ-D + Bard30 are Diabetic rats treated with Bardoxolone methyl at 15 and 30 mg/kg respectively. *$p < 0.05$, **$p < 0.01$, ***$P < 0.001$ Vs STZ-D & $^{\wedge\wedge}p < 0.01$ and $^{\wedge\wedge\wedge}p < 0.001$ Vs ND

Effect of Bard Treatment on SirT3 and LONP1 Expression

SirT3 and LONP1 expressions were significantly decreased in DRG homogenates of diabetic rats (Fig. 4) and in HG exposed PC12 cell lysates (Fig. 6B & C). Treatment with Bard dose dependently increased these protein expressions in DRG homogenates of diabetic rats (Fig. 4) and in HG exposed PC12 cell lysates (Fig. 6). Further, co-immunoprecipitation study on PC12 Cell lysates revealed that LONP1 co-expressed with SirT3 significantly decreased when compared to normal control (Fig. 4B). However, Bard treatment enhanced the LONP1 expression levels which co precipitated with SirT3 (Fig. 4B).

Effect of Bard on Total ROS Generation, Mitochondrial Superoxides and Mitochondrial Membrane Potential (Ψm)

Flow cytometry of DCFDA staining has shown significantly increased total ROS production in HG exposed PC12 cells

(Fig. 7A & B). Bard treatment at 0.5 μM concentration to HG exposed PC12 cells significantly attenuated ROS production which is evident by shifting of the histogram peak away FITC-A (green color) when compared to histogram peak of HG exposed cells as shown in the Fig. 7A. Similarly, flow cytometry of Mitosox staining has shown significantly increased mitochondrial superoxides in HG exposed PC12 cells when compared to control cells (Fig. 7C & D). Bard treatment (0.5 μM) to hyperglycemic cells displayed significantly decreased red fluorescence intensity peak as shown in the Fig. 7D which indicates decreased mitochondrial superoxides. Additionally, JC-1 staining of flow cytometry revealed that JC1 monomers were significantly predominant than JC-1 aggregates in HG exposed PC12 cells which were evident by measuring red: green fluorescence intensity ratio (Fig. 8A & B). Bard treatment significantly reversed this effect and enhanced the formation of JC-1 aggregates which is evident by increased red: green fluorescence intensity ratio (Fig. 8A & B). However, drug control has insignificant effect in altering total ROS, mitochondrial superoxides generation and mitochondrial membrane depolarization when compared to normal control group.
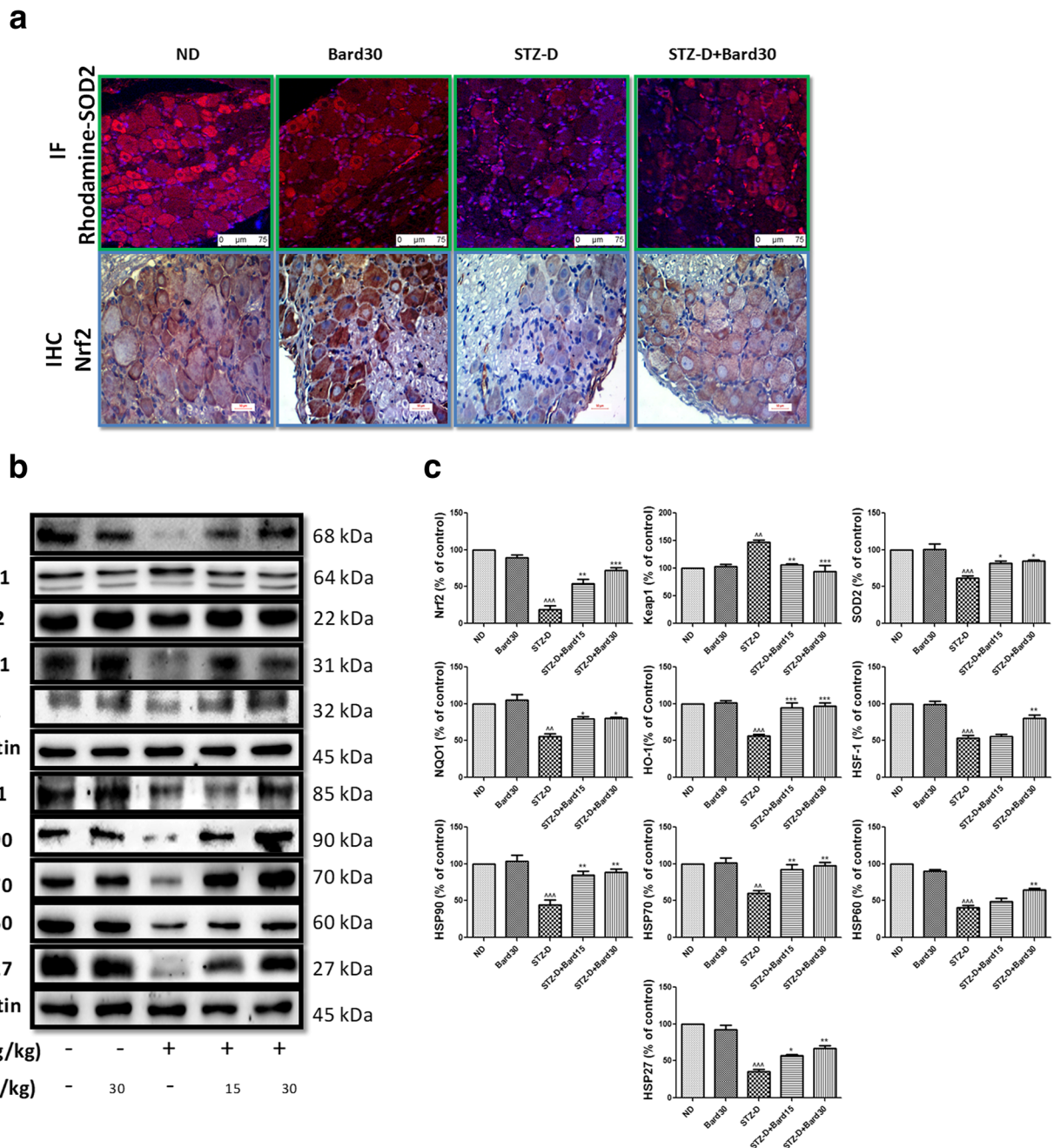
Fig. 3 Effect of Bard on antioxidant enzymes and Heat shock proteins expression in DRG homogenates of diabetic rats. (A) The upper panel shows confocal microscopic images of superoxide dismutase-2 (SOD2) immunopositivity (Red color) and the lower panel shows represents immunohistochemical expression of nuclear factor erythroid 2-related factor 2 (Nrf2) (brown color) in DRG micro sections. (B) Representative western blots and (C) respective bar graphs represent the densitometric expression of Nrf2, Keap1, SOD2, NQO1, HO-1, HSF-1, HSP90, HSP70, HSP60 and HSP27 protein expression in DRG tissue homogenates. Results are expressed as mean ± SEM (n = 3). ND: Non diabetic, Bard30: Non diabetic rats treated with Bardoxolone methyl at 30 mg/kg, STZ-D: Diabetic, STZ-D + Bard15 & STZ-D + Bard30 are Diabetic rats treated with Bardoxolone methyl at 15 and 30 mg/kg respectively. $*p < 0.05, **p < 0.01, ***P < 0.001$ Vs STZ-D & $^{\wedge\wedge}p < 0.01$ and $^{\wedge\wedge\wedge}p < 0.001$ Vs ND

Effect of Bard on Mitochondrial Function

ATP levels were significantly depleted in the freshly prepared DRG homogenate of diabetic rats when compared to control group (Fig. 5D). Bard treatment significantly enhanced ATP levels in diabetic rats in a dose dependent manner (Fig. 5D).

Moreover, immunoblotting analysis of ATP and complex I displayed dose dependent increased ATP levels in HG exposed PC12 cells when subjected to Bard treatment (Fig. 7H & I). Additionally, Bard treatment also improved mitochondrial complex activities of I, IV and V in DRG homogenates of diabetic rats (Fig. 5A, B & C) and in HG exposed PC12 cell lysates (Fig.
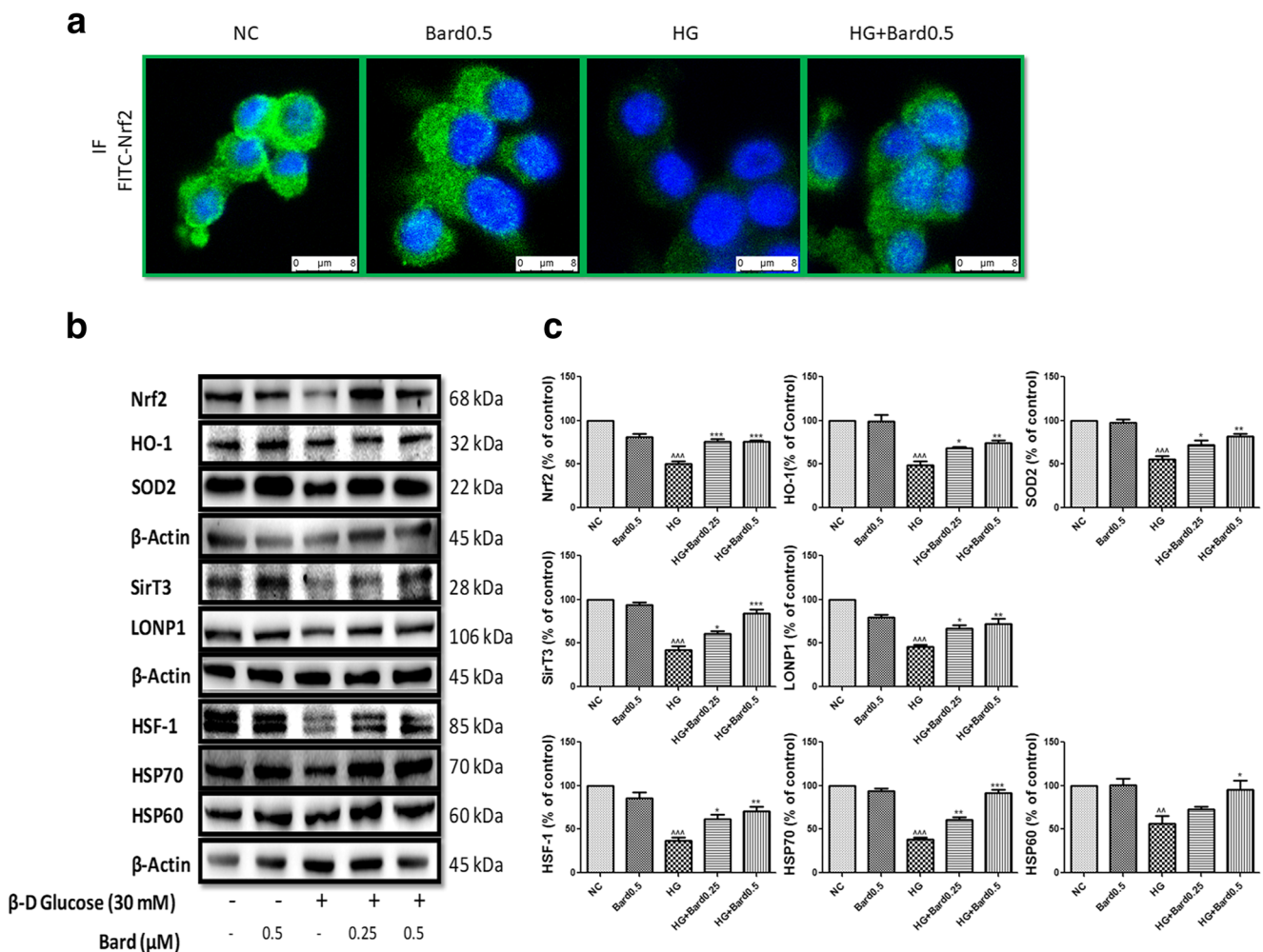
Fig. 6 **Effect of Bard on Nrf2 Immunolocalization and protein expressions in high glucose exposed PC12 cells**. (A) Confocal microscopic images showing Nrf2 Immunolocalization and expression in high glucose exposed PC12 cells (green color) and blue color represents the DAPI nuclear staining. (B) Representative western blots and (C) respective bar graphs represent the densitometric expression of Nrf2, HO-1, SOD2, SirT3, LONP1, HSF-1, HSP70 and HSP60 protein expression in PC12 cell lysates. Results are expressed as mean ± SEM (n = 3). NC: PC12 cells under basal condition, Bard0.5: Normal PC12 cells exposed to 0.5 μM Bardoxolone methyl, HG: PC12 cells exposed to 30 mM β-D Glucose, HG + Bard0.25 and HG + Bard0.5: High glucose exposed PC12 cells treated with 0.25 and 0.5 μM of Bardoxolone methyl respectively. *p < 0.05, **p < 0.01, ***P < 0.001 Vs HG & ^^p < 0.01 and ^^^p < 0.001 Vs NC

7E, F & G). These mitochondrial complex activities were compromised in DRG homogenates of diabetic rats (Fig. 5A, B & C) and in HG exposed PC12 cells (Fig. 7E, F & G). Further to corroborate these results we studied effect of Bard on OCR in PC12 cells (Fig. 8C). OCR in terms of minimal and maximal respiration, ATP production and spare respiratory capacity significantly decreased in the HG exposed PC12 cells for 24 h (Fig. 8D, E. F & G). Nrf2 activation by Bard treatment in HG exposed PC12 cells has shown significant improvement in OCR as shown in Fig. 8.

Discussion

Bard was selected as a new chemical entity under Phase 3 clinical trials for the treatment of autosomal dominant polycystic kidney disease (Clinical trial Reg ID: NCT03918447), owing to its therapeutic potentials in activating Nrf2-keap1 axis. In our previous studies, we articulated the importance of Nrf2 pathway in regulating DN [39]. Apart from our studies, other groups have also reported the role of Nrf2 and HSF1 in regulating DN [40]. However, the role of Bard in DN remains elusive and hence in the present study, we evaluated the potential of Bard treatment on various deficits associated with DN. We have found that Bard administration ameliorated DN by improving nerve functional and behavioral deficits in a dose dependent manner. Further, molecular investigations also revealed that Bard treatment improved mitochondrial function and enhanced transcriptional activity of Nrf2 and HSF-1.

In our study, Nrf2 protein expression levels were decreased in DRG of STZ induced eight weeks diabetic rats, similarly
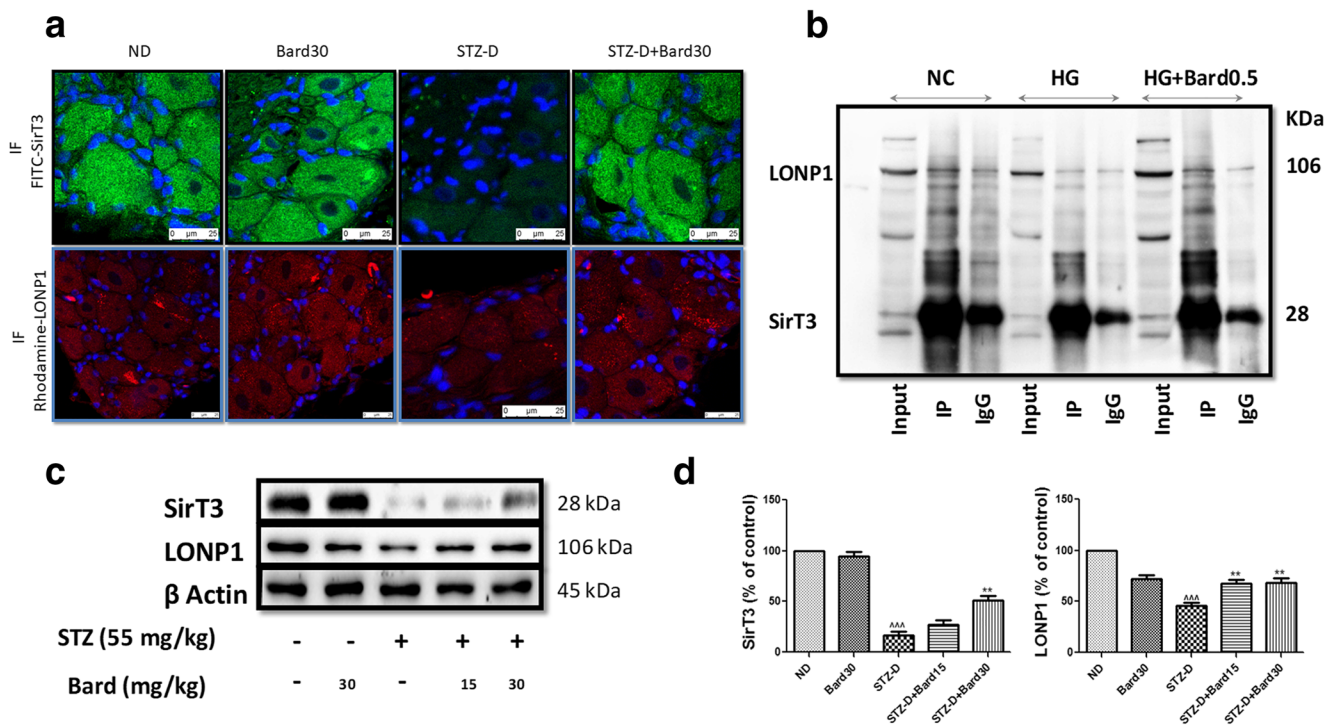
Fig. 4 Effect of Bard on SirT3 and LONP1 immunolocalization, Co-immunoprecipitation and protein expression in DRG's of STZ induced diabetic rats. (A) The upper panel shows confocal microscopic images of SirT3 immunopositivity (green color) and the lower panel shows confocal microscopic images of LONP1 immunopositivity (Red color) in DRG micro sections. (B) Co-immunoprecipitation (CO-IP) was performed in the PC12 cell lysates in NC: Normal PC12 cells, HG: high glucose exposed (30 mM) PC12 cells, HG + Bard0.5: hyperglycemic PC12 cells treated with 0.5 μM Bardoxolone methyl and IgG was used as a control for non specific signal. (C) Representative western blots and (D) respective bar graphs represent the densitometric expression of SirT3 and LONP1 protein expression in DRG tissue homogenates. Results are expressed as mean ± SEM ($n = 3$). ND: Non diabetic, Bard30: Non diabetic rats treated with Bardoxolone methyl at 30 mg/kg, STZ-D: Diabetic, STZ-D + Bard15 & STZ-D + Bard30 are Diabetic rats treated with Bardoxolone methyl at 15 and 30 mg/kg respectively. **$p < 0.01$ Vs STZ-D & ^^^$p < 0.001$ Vs ND

the translocation of Nrf2 into the nucleus was decreased in neuronal phenotype PC12 cells in response to HG stress insult. These findings were supported by many experimental and clinical studies of DN where chronic hyperglycemia resulted in depletion of Nrf2 levels and inhibition of Nrf2 translocation into the nucleus from Keap1 Protein [41–43]. In vitro and in vivo results of this study revealed Bard treatment effectively increased Nrf2 expression and downregulated Keap1 protein dose dependently and colocalization studies revealed that Nrf2 was translocated into the nucleus upon treatment with Bard. Infact, Bard forms adducts with cysteine residues of Keap1 protein and helps in releasing of Nrf2 which is hindered in the internal structure of the Keap1 [44]. Moreover, Bard treatment improved insulin resistance in high fat fed obese rats [45], protected against cisplatin induced renal toxicity, angiotensin-2 induced renal toxicity and protein overloaded nephrotoxicity by enhancing the Nrf2 expression and its translocation into the nucleus [46].

Nrf2 interacts with the two antioxidant responsive elements located between 1707 and 1530 base pairs upstream of the transcription start site of the HSF-1 gene and upregulates the expression of HSF-1 [14]. HSF-1 is considered as a stress responsive protein which plays a vital role in regulating the mitochondrial unfolded protein response. Moreover, natural phytopharmaceuticals promoting Nrf2 and HSF-1 upregulation have shown improvement in neuropathic pain from chronic diabetes [47, 48]. However, these natural compounds failed in the clinical trials owing to their poor bioavailability with assorted motives. In the current study, dose dependently Bard treatment upregulated HSF-1 in DRG homogenates of diabetic rats. We speculate this effect to the transcriptional activity of Nrf2 based on the reported literature. Bard treatment also increased the expressions of HO-1, NQO1 and SOD2 which are considered as antioxidant detoxifying enzymes in a dose dependent manner. In concurrence with our results, many studies reported that knock out or loss of these proteins expedited the neuropathic pain in different experimental models [49–51]. However, Nrf2 is considered as the master regulator of all these proteins [52]. Metabolic excess inside the neuronal cells augment the leakage of electrons from electron transport chain during the process of ATP synthesis. Recent literature evidenced mitochondrial ROS as one

Fig. 5 **Effect of Bard on ETC complex activities and ATP production in DRG's of STZ induced diabetic rats**. Bar graphs represent the (A) complex I activity (B) Complex IV activity (C) Complex V activity and (D) ATP levels in Fresh samples of DRG mitochondrial lysates. Results are expressed as mean ± SEM ($n = 3$). ND: Non diabetic, Bard30: Non diabetic rats treated with Bardoxolone methyl at 30 mg/kg, STZ-D: Diabetic, STZ-D + Bard15 & STZ-D + Bard30 are Diabetic rats treated with Bardoxolone methyl at 15 and 30 mg/kg respectively. $*p < 0.05$, $**p < 0.01$, $**p < 0.01$ Vs STZ-D & $^{\wedge\wedge\wedge}p < 0.001$ Vs ND
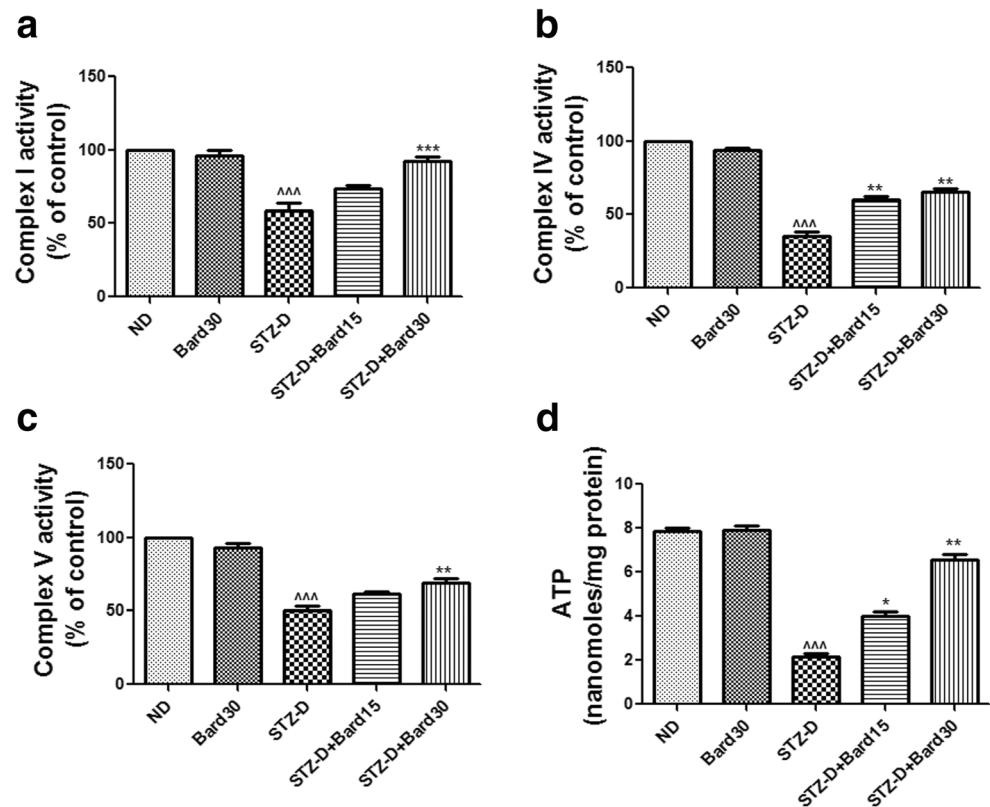
important culprit in the prognosis of diabetes induced neuronal death by accumulating oxidized proteins in the mitochondria [17]. It is reported that Nrf2 activation boost ups these antioxidant detoxifying enzymes and thereby reduces the mitochondrial and total ROS production [53]. In the current study, we witnessed that Bard treatment reduced total and mitochondrial ROS production which is in line with the published reports. Further, DRG neurons of diabetic rats also showed decreased expressions of low and high molecular weight heat shock proteins (HSP's) including HSP27, 60, 70 and 90. These HSP's were upregulated by the transcriptional activity of HSF-1 by binding at respective promoter regions of HSP genes [54]. A 13-year longitudinal study in humans, HSP27 significantly decreased from baseline in patients with type 1 diabetes and this correlated with the progression of a large fiber neuropathy [55]. In prediction of biomarkers for early detection of peripheral neuropathy, researchers found depleted levels of HSP27 in patient's blood and the patients with elevated levels of HSP27 showed reduced symptoms of neuropathic pain [56]. Number of studies reported the protective role of HSP90 in regulating the pain along with the opioids and analgesics [57]. Present study also witnessed the under expression of

HSP's which may be a reason behind developing neuropathy under hyperglycemic condition. Additionally, we also observed down regulation of SirT3 levels in DRG homogenates of diabetic rats. There are reports which evidenced that Nrf2 stimulation regulates the SirT3 expression [15]. In this study Bard treatment boosted the SirT3 expression levels in a dose dependent manner which may be driven by the activation of Nrf2. On other hand, a recent report showed that SirT3 interacts with mitochondrial lon protease (LONP1) likely at K917 site and deacetylates this ATP dependent protease [58]. Deacetylated LONP1 plays a crucial role in maintaining mitochondrial quality control by eliminating aggregated proteins and harmonizing protein turnover [17, 59]. Moreover LONP1 functions are also involved in many cellular processes - membrane fusion, protein and organelle translocation, DNA and RNA unwinding, assembly, mitochondrial DNA binding and disassembly of multi-protein complexes [60]. In consistent to these findings, we also found LONP1 was co-immunoprecipitated with SirT3 protein and Bard treatment upregulated both the proteins in DRG homogenates of diabetic rats. Despite this, mitochondrial respiration in terms of minimal respiration, maximal respiration, ATP production and spare respiratory capacity
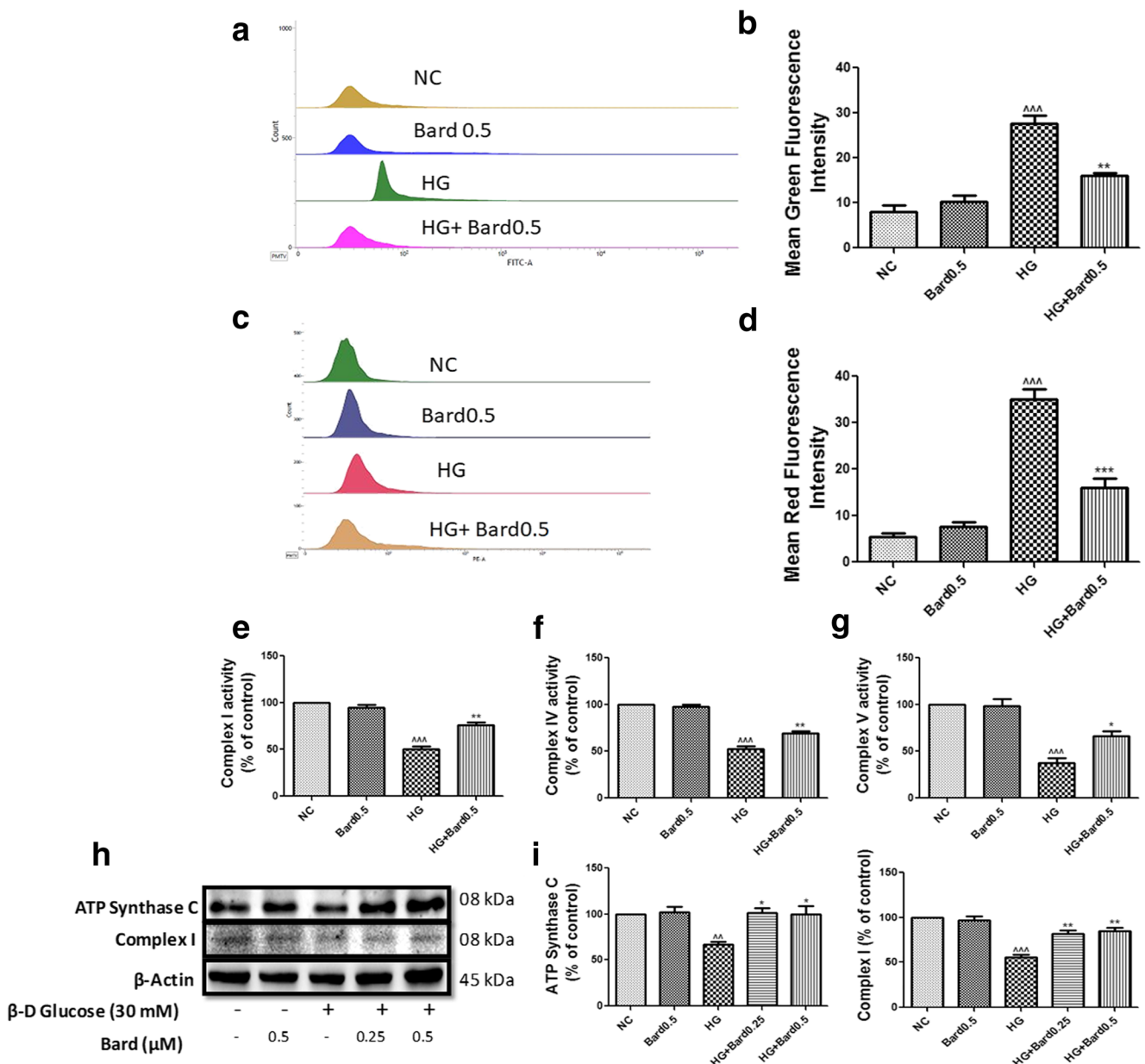
Fig. 7 Effect of Bard on Mitochondrial Function of high glucose exposed PC12 cells. (A) Representative graphs showing flow cytometric analysis of DCFDA staining indicating total ROS production in PC12 cells (C) Representative graphs showing flow cytometric analysis of Mitosox staining indicating mitochondrial superoxides production in PC12 cells and (B) & (D) Histograms represents respective quantification of green and red fluorescence intensities of DCFDA and Mitosox staining. Histograms represents (E) Complex I (F) Complex IV and (G) Complex V activities in PC12 cells mitochondrial fraction. (H) Representative western blots and (I) respective bar graphs represent the densitometric expression of ATP synthase C and Complex I protein expression in PC12 cell lysates. Results are expressed as mean ± SEM (n = 3). NC: PC12 cells under basal condition, Bard0.5: Normal PC12 cells exposed to 0.5 μM of Bardoxolone methyl, HG: PC12 cells exposed to 30 mM β-D Glucose, HG + Bard0.25 and HG + Bard0.5: High glucose exposed PC12 cells treated with 0.25 and 0.5 μM of Bardoxolone methyl respectively. *$p < 0.05$, **$p < 0.01$, ***$P < 0.001$ Vs HG & ^^^$p < 0.001$ Vs NC

were declined in high glucose exposed PC12 cells. However, Bard treatment improved mitochondrial respiration in high glucose exposed PC12 cells. Spare respiratory capacity is regarded as an important factor in defining mitochondrial function which is the actual difference between maximal and basal respiration [61].
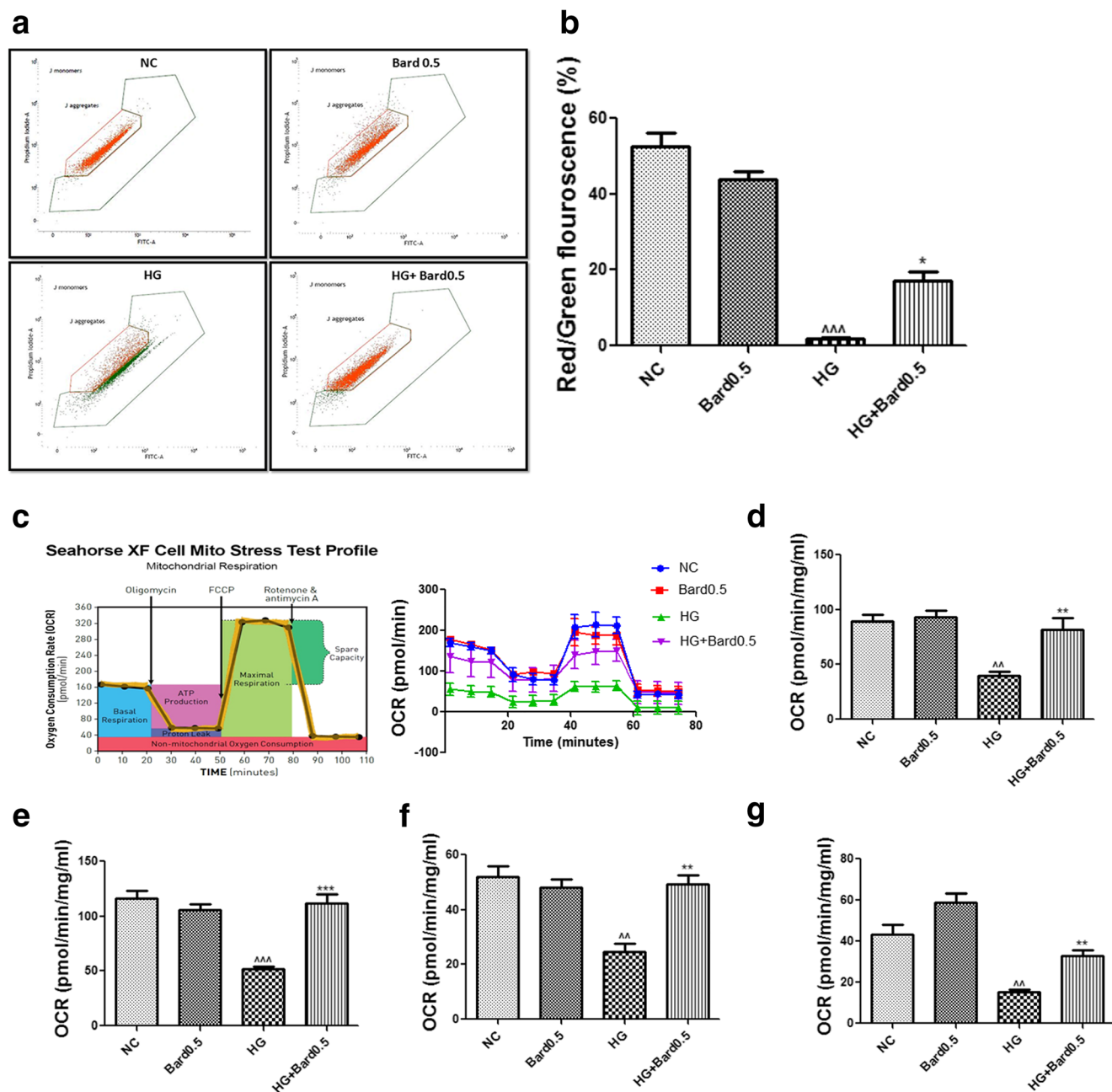
Fig. 8 Measurement of mitochondrial membrane potentials (ΔΨm) and mitochondrial respiration in cultured PC12 cells. (A) Representative dot plotted graph of JC-1 by flow cytometer represents the scattered PC12 cells into red JC-1 and green population and (B) respective quantification of red: green fluorescence ratio indicating depolarized mitochondria. (C) Oxygen consumption rate (OCR) was measured at basal level with the subsequent and sequential addition of oligomycin (1 μM), FCCP (2 μM), and rotenone+antimycin A (1 μM each) to the NC: PC12 cells under basal condition, Bard0.5: Normal PC12 cells exposed to 0.5 μM of Bardoxolone methyl, HG: PC12 cells exposed to 30 mM β-D Glucose and HG + Bard0.5: High glucose exposed PC12 cells treated with 0.5 μM of Bardoxolone methyl. The levels of OCR are normalized with per mg total protein. Agilent wave software are used to measure the OCR data and the following histograms represents the quantification of (D) basal respiration, (E) maximal respiration, (F) ATP production and (G) spare respiratory capacity. Results are expressed as mean ± SEM (n = 3). *$p < 0.05$, **$p < 0.01$, ***$P < 0.001$ Vs HG &^^$P < 0.01$, ^^^$p < 0.001$ Vs NC

In this study, when PC12 cells were subjected to hyperglycemic stress, the spare respiratory capacity declined and this energy less cells were highly susceptible to oxidative stress which later progressed to mitochondrial
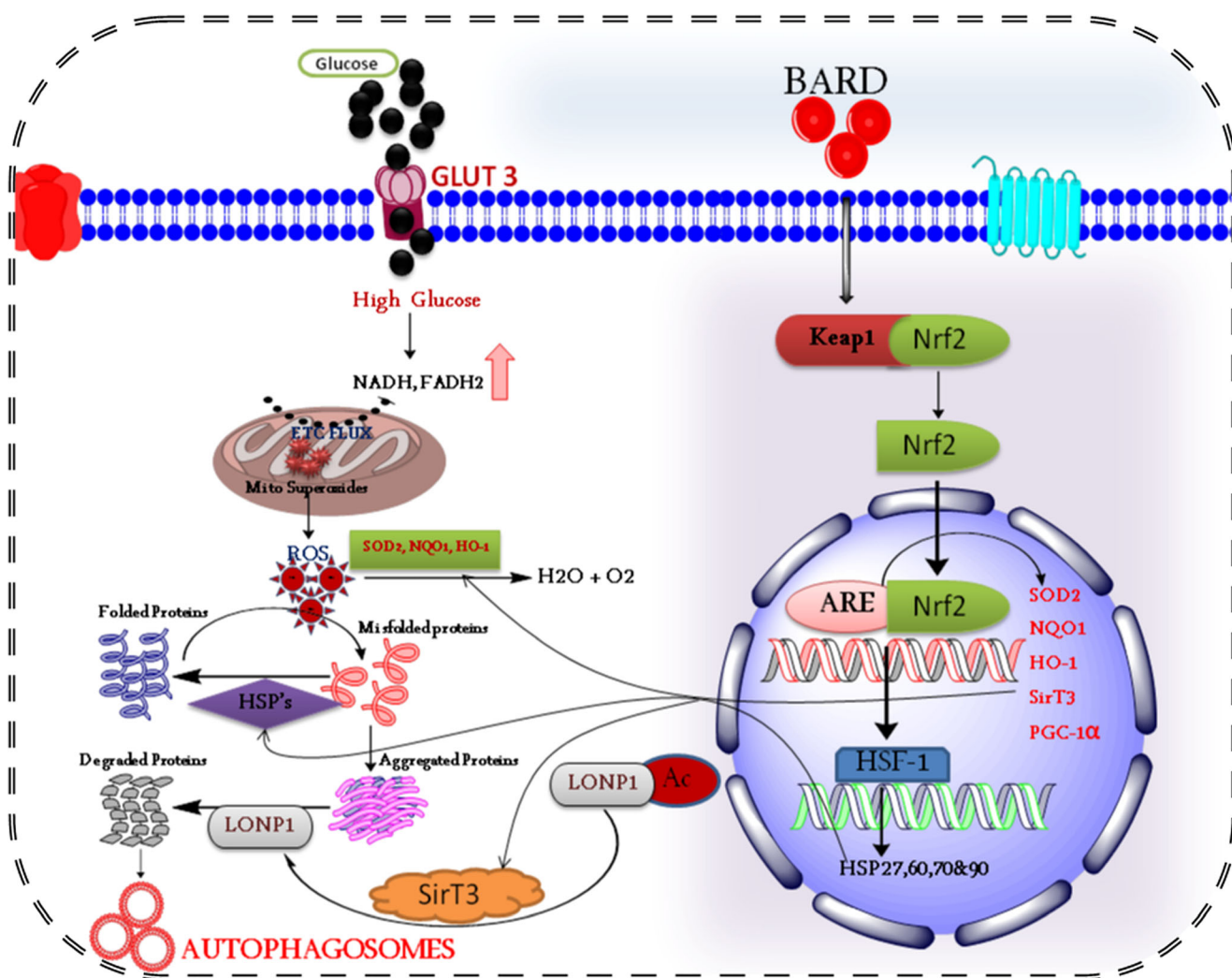
Fig. 9 Schematic diagram showing mechanistic basis for Bard mediated neuroprotection in experimental diabetic neuropathy. During chronic diabetes, excess glucose diffuses into neuronal cells through Glucose transporter 3 and this metabolic excess overloads reducing equivalents (NADH & FADH$_2$) on electron transport chain (ETC), thereby mediates excess production of mitochondrial ROS through Mitochondrial complex III. Concurrently, Mitochondrial ROS interacts with the proteins and alters the folding conformation of them. Perhaps, these misfolded proteins accumulate and forms a toxic aggregates of protein lumps. Bardoxolone methyl activates Nrf2 pathway and boost up the expressions of antioxidant defensive proteins which could scavenges free radicals, and heat shock proteins which could recuperate misfolded proteins to their normal conformation. In another hand, Nrf2 mediated SirT3 expression deacetylates the mitochondrial LON protease and that could help in removing aggregated proteins. BARD: Bardoxolone methyl, Nrf2: Nuclear factor erythroid 2-related factor 2, NQO1: NAD(P) H dehydrogenase [quinone], SOD2: Superoxide dismutase 2, HO-1: Heme oxygenase 1, HSP's: Heat shock proteins, ARE: antioxidant responsive element, SirT3: NAD-dependent deacetylase sirtuin-3, PGC-1α: Peroxisome proliferator-activated receptor gamma coactivator 1-alpha

dysfunction. Bard treatment by stimulating Nrf2-ARE axis enhanced spare respiratory capacity which boosted the function of mitochondria.

Conclusion

The results obtained from our studies suggest that Bard may alleviate experimental DN by enhancing the levels of antioxidant defense enzymes, improving chaperone and protease activity and boosting mitochondrial respiration via stimulation of Nrf2-ARE

pathway. Our studies thus offer novel insights to understand the mechanism of action of Bard as a neuroprotective agent, and to identify novel targets for the pharmacological management of DN.

Author's Contributions Mr. Anil Kumar Kalvala (Department of Pharmacology and Toxicology, NIPER-HYDERABAD, Telangana, India - 500,037), Performed studies, evaluated data, prepared figures

Compliance with Ethical Standards

Conflict of Interest The authors declare that there are no conflicts of interest.

References

1. Ahmad A, Hussain A, Baig MAR, Arain SA (2019) Diabetes mellitus; prevalence of undiagnosed diabetes mellitus in patients of acute myocardial infraction. Professional Med 26(2)

2. Bruschi LKM, da Rocha DA, Gesteira Filho EL, Barboza NMP, Frisanco PAB, Callegaro RM, de Sá LBPC, Arbex AK (2017) Diabetes mellitus and diabetic peripheral neuropathy. Open J Endocr Metab Dis 7(1):12–21

3. Amin DAeS (2016) Knowledge and practices of type II diabetic patients' regarding diabetic foot self-care and their foot disorders. ZNJ 12 (1):18–35

4. Lindsay TJ, Rodgers BC, Savath V, Hettinger KD (2010) Treating diabetic peripheral neuropathic pain. Am Fam Physician 82(2): 151–158

5. Kalvala AK, Yerra VG, Kumar A (2020) LONP1 induction by SRT1720 attenuates mitochondrial dysfunction against high glucose induced neurotoxicity in PC12 cells. Toxicol in Vitro 62: 104695

6. Fernyhough P (2015) Mitochondrial dysfunction in diabetic neuropathy: A series of unfortunate metabolic events. Curr Diab Rep 15(11):89

7. Russel JW, Golovoy D, Vincent AM, Mahendru P, Olzmann JA, Mentzer A, Feldman EL (2002) High glucose-induced oxidative stress and mitochondrial dysfunction in neurons. FASEB J 16(13):1738–1748

8. Gureev AP, Shaforostova EA, Popov VN (2019) Regulation of mitochondrial biogenesis as a way for active longevity: Interaction between the Nrf2 and PGC-1α signaling pathways. Front Genet 10:435

9. Joe Y, Zheng M, Kim HJ, Uddin MJ, Kim S-K, Chen Y, Park J, Cho GJ et al (2015) Cilostazol attenuates murine hepatic ischemia and reperfusion injury via heme oxygenase-dependent activation of mitochondrial biogenesis. Am J Physiol-Gastr L 309(1):G21–G29

10. Athale J, Ulrich A, MacGarvey NC, Bartz RR, Welty-Wolf KE, Suliman HB, Piantadosi CA (2012) Nrf2 promotes alveolar mitochondrial biogenesis and resolution of lung injury in Staphylococcus aureus pneumonia in mice. Free Radic Biol Med 53(8):1584–1594

11. Kadıoğlu E, Tekşen Y, Koçak C, Koçak FE (2019) Beneficial effects of bardoxolone methyl, an Nrf2 activator, on crush-related acute kidney injury in rats. Eur J trauma Emerg S:1-10

12. Pergola PE, Krauth M, Huff JW, Ferguson DA, Ruiz S, Meyer CJ, Warnock DG (2011) Effect of bardoxolone methyl on kidney function in patients with T2D and stage 3b–4 CKD. Am J Nephrol 33(5):469–476

13. Naidu SD, Dinkova-Kostova AT (2017) Regulation of the mammalian heat shock factor 1. FEBS J 284(11):1606–1627

14. Paul S, Ghosh S, Mandal S, Sau S, Pal M (2018) NRF2 transcriptionally activates the heat shock factor 1 promoter under oxidative stress and affects survival and migration potential of MCF7 cells. J Biol Chem 293(50):19303–19316

15. Marcus JM, Andrabi SA (2018) SIRT3 regulation under cellular stress: Making sense of the ups and downs. Front Neurosci 12:799

16. Satterstrom FK, Swindell WR, Laurent G, Vyas S, Bulyk ML, Haigis MC (2015) Nuclear respiratory factor 2 induces SIRT 3 expression. Aging Cell 14(5):818–825

17. Kalvala AK, Khan I, Gundu C, Kumar A (2019) An overview on ATP dependent and independent proteases including an anterograde to retrograde control on mitochondrial function; focus on diabetes and diabetic complications. Curr Pharm Des 25(23): 2584–2594

18. Bota DA, Davies KJ (2016) Mitochondrial Lon protease in human disease and aging: Including an etiologic classification of Lon-related diseases and disorders. Free Radic Biol Med 100:188–198

19. Yerra VG, Kalvala AK, Kumar A (2017) Isoliquiritigenin reduces oxidative damage and alleviates mitochondrial impairment by SIRT1 activation in experimental diabetic neuropathy. J Nutr Biochem 47:41–52

20. Liu M, Reddy NM, Higbee EM, Potteti HR, Noel S, Racusen L, Kensler TW, Sporn MB et al (2014) The Nrf2 triterpenoid activator, CDDO-imidazolide, protects kidneys from ischemia–reperfusion injury in mice. Kidney Int 85(1):134–141

21. Pergola PE, Krauth M, Huff JW, Ferguson DA, Ruiz S, Meyer CJ, Warnock DG (2011) Effect of bardoxolone methyl on kidney function in patients with T2D and stage 3b–4 CKD. Am J Nephrol 33(5):469–476

22. De Zeeuw D, Akizawa T, Audhya P, Bakris GL, Chin M, Christ-Schmidt H, Goldsberry A, Houser M et al (2013) Bardoxolone methyl in type 2 diabetes and stage 4 chronic kidney disease. N Engl J Med 369(26):2492–2503

23. Chin MP, Bakris GL, Block GA, Chertow GM, Goldsberry A, Inker LA, Heerspink HJ, O'Grady M et al (2018) Bardoxolone methyl improves kidney function in patients with chronic kidney disease stage 4 and type 2 diabetes: Post-hoc analyses from bardoxolone methyl evaluation in patients with chronic kidney disease and type 2 diabetes study. Am J Nephrol 47(1):40–47

24. Chin MP, Reisman SA, Bakris GL, O'grady M, Linde PG, McCullough PA, Packham D, Vaziri ND et al (2014) Mechanisms contributing to adverse cardiovascular events in patients with type 2 diabetes mellitus and stage 4 chronic kidney disease treated with bardoxolone methyl. Am J Nephrol 39(6): 499–508

25. Thimmulappa RK, Fuchs RJ, Malhotra D, Scollick C, Traore K, Bream JH, Trush MA, Liby KT et al (2007) Preclinical evaluation of targeting the Nrf2 pathway by triterpenoids (CDDO-Im and CDDO-me) for protection from LPS-induced inflammatory response and reactive oxygen species in human peripheral blood mononuclear cells and neutrophils. Antioxid Redox Sign 9(11): 1963–1970

26. Kocak C, Kocak FE, Akcilar R, Bayat Z, Aras B, Metineren MH, Yucel M, Simsek H (2016) Effects of captopril, telmisartan and bardoxolone methyl (CDDO-me) in ischemia-reperfusion-induced acute kidney injury in rats: An experimental comparative study. Clin Exp Pharmacol Physiol 43(2):230–241

27. Yerra VG, Kumar A (2017) Adenosine monophosphate-activated protein kinase abates hyperglycaemia-induced neuronal injury in experimental models of diabetic neuropathy: Effects on

mitochondrial biogenesis, autophagy and neuroinflammation. Mol Nerobiol 54(3):2301–2312

28. Rosenblum BR, Bonner RF, Oldfield EH (1987) Intraoperative measurement of cortical blood flow adjacent to cerebral AVM using laser Doppler velocimetry. J Neurosurg 66(3):396–399

29. Ma Z, Li Y, Zhang YP, Shields LB, Xie Q, Yan G, Liu W, Chen G et al (2015) Thermal nociception using a modified Hargreaves method in primates and humans. Funct Neurol 30(4):229–236

30. Kumar A, Kaundal RK, Iyer S, Sharma SS (2007) Effects of resveratrol on nerve functions, oxidative stress and DNA fragmentation in experimental diabetic neuropathy. Life Sci 80(13):1236–1244

31. Sandireddy R, Yerra VG, Komirishetti P, Areti A, Kumar A (2016) Fisetin imparts neuroprotection in experimental diabetic neuropathy by modulating Nrf2 and NF-κB pathways. Cell Mol Neurobiol 36(6):883–892

32. Areti A, Komirishetty P, Akuthota M, Malik RA, Kumar A (2017) Melatonin prevents mitochondrial dysfunction and promotes neuroprotection by inducing autophagy during oxaliplatin-evoked peripheral neuropathy. J Pineal Res 62(3):e12393

33. Yerra VG, Kalvala AK, Sherkhane B, Areti A, Kumar A (2018) Adenosine monophosphate-activated protein kinase modulation by berberine attenuates mitochondrial deficits and redox imbalance in experimental diabetic neuropathy. Neuropharmacology 131:256–270

34. Lips K, Pfeil U, Kummer W (2002) Coexpression of α9 and α10 nicotinic acetylcholine receptors in rat dorsal root ganglion neurons. Neuroscience 115(1):1–5

35. Bachewal P, Gundu C, Yerra VG, Kalvala AK, Areti A, Kumar A (2018) Morin exerts neuroprotection via attenuation of ROS induced oxidative damage and neuroinflammation in experimental diabetic neuropathy. Biofactors 44(2):109–122

36. Gunjan S, Sharma T, Yadav K, Chauhan BS, Singh SK, Siddiqi MI, Tripathi R (2018) Artemisinin derivatives and synthetic trioxane trigger apoptotic cell death in asexual stages of plasmodium. Front Cell Infect Microbiol 8:256

37. Resham K, Sharma SS (2019) Pharmacologic inhibition of porcupine, disheveled, and β-catenin in Wnt signaling pathway ameliorates diabetic peripheral neuropathy in rats. J Pain 20(11):1338–1352

38. Thatikonda S, Pooladanda V, Sigalapalli DK, Godugu C (2020) Piperlongumine regulates epigenetic modulation and alleviates psoriasis-like skin inflammation via inhibition of hyperproliferation and inflammation. Cell Death Dis 11(1):1–17

39. Arruri V, Komirishetty P, Areti A, Dungavath SKN, Kumar A (2017) Nrf2 and NF-κB modulation by Plumbagin attenuates functional, behavioural and biochemical deficits in rat model of neuropathic pain. Pharmacol Rep 69(4):625–632

40. Dobrowsky RT (2016) Targeting the diabetic chaperome to improve peripheral neuropathy. Curr Diab Rep 16(8):71

41. Negi G, Kumar A, Sharma SS (2011) Melatonin modulates neuroinflammation and oxidative stress in experimental diabetic neuropathy: Effects on NF-κB and Nrf2 cascades. J Pineal Res 50(2):124–131

42. Liu Y-W, Cheng Y-Q, Liu X-L, Hao Y-C, Li Y, Zhu X, Zhang F, Yin X-X (2017) Mangiferin upregulates glyoxalase 1 through activation of Nrf2/ARE signaling in central neurons cultured with high glucose. Mol Neurobiol 54(6):4060–4070

43. Jiménez-Osorio AS, Picazo A, González-Reyes S, Barrera-Oviedo D, Rodríguez-Arellano ME, Pedraza-Chaverri J (2014) Nrf2 and redox status in prediabetic and diabetic patients. Int J Mol Sci 15(11):20290–20305

44. Wu J, Liu X, Fan J, Chen W, Wang J, Zeng Y, Feng X, Yu X et al (2014) Bardoxolone methyl (BARD) ameliorates aristolochic acid (AA)-induced acute kidney injury through Nrf2 pathway. Toxicology 318:22–31

45. Dinh CH, Szabo A, Yu Y, Camer D, Wang H, Huang X-F (2015) Bardoxolone methyl prevents mesenteric fat deposition and inflammation in high-fat diet mice. Sci World J 2015:1–15

46. Wang Y-Y, Yang Y-X, Zhe H, He Z-X, Zhou S-F (2014) Bardoxolone methyl (CDDO-me) as a therapeutic agent: An update on its pharmacokinetic and pharmacodynamic properties. Drug Des Dev Ther 8:2075

47. Matzinger M, Fischhuber K, Heiss EH (2018) Activation of Nrf2 signaling by natural products-can it alleviate diabetes? Biotechnol Adv 36(6):1738–1767

48. Verma P, Pfister JA, Mallick S, D'Mello SR (2014) HSF1 protects neurons through a novel trimerization-and HSP-independent mechanism. J Neurosci 34(5):1599–1612

49. Oh SS, Sullivan KA, Wilkinson JE, Backus C, Hayes JM, Sakowski SA, Feldman EL (2012) Neurodegeneration and early lethality in superoxide dismutase 2-deficient mice: A comprehensive analysis of the central and peripheral nervous systems. Neuroscience 212:201–213

50. Negi G, Nakkina V, Kamble P, Sharma SS (2015) Heme oxygenase-1, a novel target for the treatment of diabetic complications: Focus on diabetic peripheral neuropathy. Pharmacol Res 102:158–167

51. Stringer JL, Gaikwad A, Gonzales BN, Long DJ Jr, Marks LM, Jaiswal AK (2004) Presence and induction of the enzyme NAD (P) H: Quinone oxidoreductase 1 in the central nervous system. J Comp Neurol 471(3):289–297

52. Li W, Kong AN (2009) Molecular mechanisms of Nrf2-mediated antioxidant response. Molecular Carcinogenesis: Published in cooperation with the University of Texas MD Anderson Cancer Center 48(2):91–104

53. Dinkova-Kostova AT, Abramov AY (2015) The emerging role of Nrf2 in mitochondrial function. Free Radic Biol Med 88:179–188

54. Zheng X, Krakowiak J, Patel N, Beyzavi A, Ezike J, Khalil AS, Pincus D (2016) Dynamic control of Hsf1 during heat shock by a chaperone switch and phosphorylation. Elife 5:e18638

55. Pourhamidi K, Skärstrand H, Dahlin LB, Rolandsson O (2014) HSP27 concentrations are lower in patients with type 1 diabetes and correlate with large nerve fiber dysfunction. Diabetes Care 37(3):e49–e50

56. Pourhamidi K, Dahlin LB, Boman K, Rolandsson O (2011) Heat shock protein 27 is associated with better nerve function and fewer signs of neuropathy. Diabetologia 54(12):3143–3149

57. Nascimento DSM, Potes CS, Soares ML, Ferreira AC, Malcangio M, Castro-Lopes JM, Neto FLM (2018) Drug-induced HSP90 inhibition alleviates pain in monoarthritic rats and alters the expression of new putative pain players at the DRG. Mol Neurobiol 55(5):3959–3975

58. Gibellini L, Pinti M, Beretti F, Pierri CL, Onofrio A, Riccio M, Carnevale G, De Biasi S et al (2014) Sirtuin 3 interacts with Lon protease and regulates its acetylation status. Mitochondrion 18:76–81

59. Hannah-Shmouni F, MacNeil L, Brady L, Nilsson MI, Tarnopolsky M (2019) Expanding the clinical spectrum of LONP1-related mitochondrial cytopathy. Front Neurol 10

60. Lee SR, Han J (2017) Mitochondrial nucleoid: shield and switch of the mitochondrial genome Oxidative med cell longev:2017

61. Yamamoto H, Morino K, Mengistu L, Ishibashi T, Kiriyama K, Ikami T, Maegawa H (2016) Amla enhances mitochondrial spare respiratory capacity by increasing mitochondrial biogenesis and antioxidant systems in a murine skeletal muscle cell line Oxid Med Cell Longev:2016